

Quantum ergodicity in the many-body localization problem

Felipe Monteiro,¹ Masaki Tezuka,² Alexander Altland,³ David A. Huse,⁴ and T. Micklitz¹

¹*Centro Brasileiro de Pesquisas Físicas, Rua Xavier Sigaud 150, 22290-180, Rio de Janeiro, Brazil*

²*Department of Physics, Kyoto University, Kyoto 606-8502, Japan*

³*Institut für Theoretische Physik, Universität zu Köln, Zùlpicher Str. 77, 50937 Cologne, Germany*

⁴*Department of Physics, Princeton University, Princeton, NJ 08544, USA*

(Dated: February 26, 2022)

We generalize Page’s result on the entanglement entropy of random pure states to the many-body eigenstates of realistic disordered many-body systems subject to long range interactions. This extension leads to two principal conclusions: first, for increasing disorder the “shells” of constant energy supporting a system’s eigenstates fill only a fraction of its full Fock space and are subject to intrinsic correlations absent in synthetic high-dimensional random lattice systems. Second, in all regimes preceding the many-body localization transition individual eigenstates are thermally distributed over these shells. These results, corroborated by comparison to exact diagonalization for an SYK model, are at variance with the concept of “non-ergodic extended states” in many-body systems discussed in the recent literature.

PACS numbers: 05.45.Mt, 72.15.Rn, 71.30.+h

Introduction:— Complex quantum systems exposed to external disorder may enter a phase of strong localization. About two decades after the prediction of many-body localization (MBL) [1, 2, 38], there is still no strong consensus about the stability of the MBL phase and/or the possible presence of an intermediate phase between MBL and the thermal phase. One class of models where these questions can be explored with more analytic control is confined many-body systems with long-range interactions. Under these conditions, the interaction operator couples all single-particle states, which facilitates the analysis. At the same time, the Hilbert space dimension is still exponentially large in the particle number, which leads to rich physics relevant to systems such as chaotic many body quantum devices [4–8], small sized optical lattices [9–11], or qubit arrays [12, 13].

In recent years, the complex structure of many-body quantum *states* in MBL has become a focus of intensive research. Unlike with single particle problems, where extended wave functions uniformly cover real space, increasing the disorder in a phase of extended many body states $|\psi\rangle$ leads to a diminished wave function support in Fock space. This phenomenon, which shows, e.g., in a suppression of wave function moments (WFM) $|\langle n|\psi\rangle|^{2q}$ in an occupation number basis, $|n\rangle$, has led to the proposal of a phase of “*nonergodic* extended states” [14–17] intermediate between the phases of absent and strong localization. An alternative scenario is that for each realization of the disorder only a subset of states $\{|n\rangle\}$ have finite overlap with the eigenstates of energy E , and in this way define a quantum *energy shell* in Fock space. A uniform (thermal) distribution of the exact eigenstates on this shell would then be the defining criterion for maintained quantum *ergodicity* on the delocalized side of the MBL transition.

At this stage, there is mounting evidence in favor of

the second scenario [18–21]. However, in order to firmly characterize the physics of a globally realized many body ergodic quantum phase, two questions need to be addressed: how can the energy shell be described in quantitative terms? And what is the distribution of quantum states on that shell? As indicated above, wave function statistics can provide at least part of an answer to the first question. In this Letter, we focus on the equally important second part of the problem and demonstrate that the key to its solution lies in concepts of quantum information. Specifically, we will compute pure state entanglement entropies (EE) under a relatively mild set of assumptions. Within this framework we find that to zeroth order wave functions remain thermally distributed over the shell. This establishes a microcanonical distribution, in agreement with the second scenario — maintained ergodicity in all regimes prior to the transition. In addition, the EE contains sub-leading terms which reflect the characteristic way in which the energy shell is interlaced into Fock space. These contributions sharply distinguish the energy shells of genuine many body systems from those of phenomenological high dimensional models such as the random energy model (REM), or sparse random states [22]. In this way the combined analysis of WFMs and EEs becomes a sensitive probe into the complex manifestation of wave function ergodicity in many particle systems.

Pure state entanglement entropies: — For a pure state, $\rho = |\psi\rangle\langle\psi|$, the entanglement entropy relative to a partitioning $\mathcal{F} = \mathcal{F}_A \otimes \mathcal{F}_B$ of Fock space is defined as the von Neumann entropy, $S_A = -\text{tr}_A(\rho_A \ln \rho_A)$ of the reduced density matrix $\rho_A = \text{tr}_B(|\psi\rangle\langle\psi|)$. The entanglement entropies of pure maximally random states were calculated in the classic Ref. [23]. More recent work [24] emphasizes the utility of the concept in the context of random matrix models serving as proxies of high-dimensional lo-

calizing systems [15]. In these systems, quantum interference shows in a contribution to the entanglement entropy proportional to the ratio of subsystem Fock-space dimensions. A main finding of the present work is that energy-shell correlations distinguishing microscopic systems from random matrix models open a second channel of quantum information and exponentially enhance the suppression of the entanglement below its thermal value. In this way, the entanglement sharply distinguishes between genuine many-body wave functions and wave functions on generic high-dimensional random lattices.

In the rest of this Letter, we will compute the entanglement entropy of pure states prior to the onset of strong localization under a minimal set of assumptions. We will compare our results to the entropies obtained for phenomenological models and to numerical data obtained for a Majorana SYK model.

Energy shell: — We begin with a qualitative discussion of the Fock space energy shell. Consider a many-body Hamiltonian $\hat{H} = \hat{H}_2 + \hat{H}_4$, where \hat{H}_4 is an interaction operator and \hat{H}_2 a one-body operator defined by a single particle spectrum $\{m_i\}$, $i = 1, \dots, N$ distributed over a range δ . Working in the eigenbasis of \hat{H}_2 , Fock space is spanned by the $D \equiv 2^N$ occupation number states $n = (n_1, \dots, n_N)$, $n_i = 0, 1$ for spinless fermions. We interpret these states as sites of a hypercubic lattice, carrying local potentials $v_n = \sum (2n_i - 1)m_i$ with r.m.s. value $\Delta_2 \equiv N^{1/2}\delta$. Individual states n are connected to a polynomially large number N^α of ‘nearest neighbors’ m by the interaction \hat{H}_4 . For interaction matrix elements $t_{nm} \sim gN^{-\beta/2}$, the r.m.s. eigenvalue of \hat{H}_4 scales as $\Delta_4 \sim gN^{(\alpha-\beta)/2}$, with g an N -independent coupling energy for the interaction. These interactions change only an order-one number of occupation numbers, so $|v_n - v_m|$ is of order δ and thus for large N much smaller than the ‘bandwidth’ Δ_2 of \hat{H}_2 .

In the competition of the operators \hat{H}_2 and \hat{H}_4 , states n may hybridize with states m via the coupling t_{nm} . When the eigenstates of \hat{H} are delocalized in Fock space, this hybridization gives the local spectral density

$$\nu_n(E) \equiv -\frac{1}{\pi} \text{Im} \langle n | (E^+ - \hat{H})^{-1} | n \rangle, \quad (1)$$

a linewidth $\kappa = \kappa(v_n, \delta, g)$ which must be self-consistently determined [25]. The solution of Eq. (1) for a given realization of the disorder contains the essential information on the distribution of the energy shell in Fock space. Specifically, for generic values of the energy E (we set $E = 0$ for concreteness), the strength of the disorder, δ , defines four regimes of different shell structure:

I: $\delta \ll N^{-1/2}\Delta_4$: the characteristic disorder band width $\delta N^{1/2} = \Delta_2 \ll \Delta_4$ is perturbatively small. In this regime, the spectral density, $\nu_n \equiv \nu$ is approximately constant over energy scales $\sim \Delta_2$.

II: $N^{-1/2}\Delta_4 \ll \delta \ll \Delta_4$: the bandwidth of \hat{H}_2 exceeds that of the interaction \hat{H}_4 , but nearest neighbors remain

energetically close $|v_n - v_m| \sim \delta \ll \Delta_4$. In this regime, $\kappa = \Delta_4$, indicating that the full interaction Hamiltonian enters the hybridization of neighboring sites.

III: $\Delta_4 \ll \delta \ll \delta_c$: only a fraction $\sim (\Delta_4/\delta)^2$ of nearest neighbors remain in resonance, and the broadening is reduced to $\kappa \sim \Delta_4^2/\delta$.

IV: The threshold to localization, δ_c , is reached when less than one of the $\sim N^\alpha$ neighbors of characteristic energy separation δ falls into the broadened energy window. Up to corrections logarithmic in N (and neglecting potential modifications due to Fock space loop amplitudes) this leads to the estimate $\delta_c \sim N^{\alpha/2}\Delta_4$ for the boundary to the strong localization regime.

The energy shell in the delocalized regimes II and III is an extended cluster of resonant sites embedded in Fock space. It owes its structure to the competition between the large number $\mathcal{O}(N^\alpha)$ of nearest neighbor matrix elements and the detuning of statistically correlated nearest neighbor energies, v_n, v_m . In regime II, only a polynomially (in N) small fraction $\kappa/\Delta_2 \stackrel{II}{\sim} \Delta_4/(\delta N^{1/2})$ of Fock space sites lie in the resonant window defining the energy shell, and in III this fraction is further reduced to $\stackrel{III}{\sim} \Delta_4^2/(\delta^2 N^{1/2})$, before the shell fragments at the boundary to regime IV.

We also note that if a site, n , lies on the shell, the probability that its neighboring sites of energy $v_m = v_n \pm \mathcal{O}(\delta)$ are likewise on-shell is parametrically enhanced compared to that of generic sites with energy $v_n \pm \mathcal{O}(\Delta_2)$. It is this principle which gives the energy shell of many-body systems a high degree of internal correlations (absent in phenomenological lattice models with statistically independent on-site randomness) [26]. What physical quantities are sensitive to these correlations? And how do quantum states spread over the shell structure? As we are going to discuss next, the pure state entanglement entropy, S_A , contains the answer to these questions.

Entanglement entropy: — Consider a Fock space (outer product) partitioning defined by $n = (l, m)$ where the N_A -bit vector l labels the states of subsystem A and m those of B with $N_B = N - N_A \gg N_A$. We are interested in the disorder averaged moments $M_r \equiv \langle \text{tr}_A(\rho_A^r) \rangle$, and the entanglement entropy $S_A = -\partial_r M_r|_{r=1}$ of the reduced density matrix, $\rho_A = \text{tr}_B(|\psi\rangle\langle\psi|)$, defined by a realization-specific zero-energy eigenstate $\hat{H}|\psi\rangle = 0$. The bookkeeping of index configurations entering the moments $\text{tr}_A(\rho_A^r) = \psi_{l^1 m^1} \bar{\psi}_{l^2 m^1} \psi_{l^2 m^2} \dots \psi_{l^r m^r} \bar{\psi}_{l^1 m^r}$ is conveniently done in a tensor network representation as in Fig. 1. Introducing a multi-index $\mathcal{N} \equiv (n^1, \dots, n^r)$, and analogously for $\mathcal{N}_{A,B}$, the figure indicates how the index-data \mathcal{N} and \mathcal{M} carried by ψ and $\bar{\psi}$ is constrained by the summation as $\mathcal{M}_B^i = \mathcal{N}_B^i$ and $\mathcal{M}_A^i = \mathcal{N}_A^{\tau i}$, where $\tau i = (i+1) \bmod(r)$. A further constraint, indicated by red lines in the bottom part of the figure, arises from the random phase cancellation under averaging, which in the present notation requires $\mathcal{N}^i \equiv \mathcal{M}^{\sigma i}$, for *some*

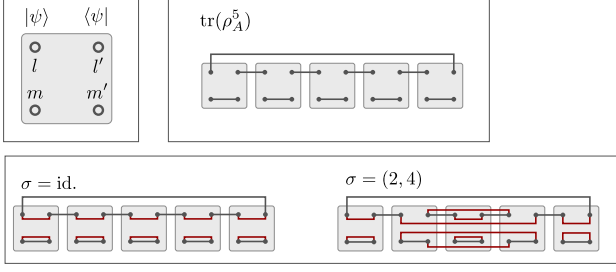


FIG. 1: Top left: graphic representation of the tensor amplitude $\psi_{lm}\bar{\psi}_{l'm'}$. Top right: contraction of indices defining $\text{tr}(\rho_A^5)$. Bottom: averaging enforces pairwise equality of indices n, n' in tensor products $\langle \dots \psi_n \dots \bar{\psi}_{n'} \dots \rangle$, as indicated by red lines. Left: identity pairing of indices within the five factors $\langle \text{tr}_A(\rho_A \rho_A \rho_A \rho_A \rho_A) \rangle$. Right: pairing of indices of the second and fourth factor.

permutation σ . (The figure illustrates this for the identity, $\sigma = \text{id.}$, and the transposition $\sigma = (2, 4)$.) Combining the two constraints, we obtain the representation $M_r = \sum_{\sigma} \sum_{\mathcal{N}} \prod_i \langle |\psi_{n_i}|^2 \rangle \delta_{\mathcal{N}_A, (\sigma \circ \tau) \mathcal{N}_A} \delta_{\mathcal{N}_B, \sigma \mathcal{N}_B}$. This expression is universal in that it does not require assumptions other than the random phase cancellation. In a less innocent final step we establish contact to the previously discussed local density of states, ν_n , and compare the two representations $D\nu \equiv \sum_{\alpha} \delta(E - E_{\alpha}) = \sum_{n, \alpha} |\psi_{\alpha, n}|^2 \delta(E - E_{\alpha}) = \sum_n \nu_n$ to identify $|\psi_n|^2 = \frac{\nu_n}{D\nu}$. In other words, we identify the moduli $|\psi_n|^2$ of a fixed eigenstate $\psi = \psi_{\alpha}$ with the realization specific local density of states, ν_n , at $E = E_{\alpha}$. For the legitimacy of this replacement for single particle random systems see Ref. [30], and for the SYK model the Supplemental Material and Ref. [31]. With this substitution, we obtain the representation

$$M_r = \sum_{\sigma} \sum_{\mathcal{N}} \prod_{i=1}^r \lambda_{n_i} \delta_{\mathcal{N}_A, (\sigma \circ \tau) \mathcal{N}_A} \delta_{\mathcal{N}_B, \sigma \mathcal{N}_B}, \quad (2)$$

with $\lambda_n \equiv \frac{\nu_n}{D\nu}$. This expression describes two complementary perspectives of quantum states in Fock space: their support on a random energy shell defined by the coefficients $\lambda_n \sim \nu_n$, and random phase cancellations implicit in the combinatorial structure. In the following, we discuss the manifestations of these principles in the above regimes I-IV.

Regime I, maximally random states: — Here, wave functions are uniformly distributed, $\nu_n = \nu$, and the evaluation of Eq. (2) reduces to a combinatorial problem. The latter has been addressed in the string theory literature [32, 33] (where high-dimensional pure random states are considered as proxies for black hole micro states.) Inspection of the formula shows that increasing permutation complexity needs to be paid for in summation factors D_B . Keeping only the leading term, $\sigma = \text{id.}$, and the next leading single transpositions $\sigma = (ij)$, we

obtain $M_r \approx D_A^{1-r} + \binom{r}{2} D_A^{2-r} D_B^{-1}$, and the subsequent differentiation in r yields Page's result [23]

$$S_A - S_{\text{th}} = -\frac{D_A}{2D_B}, \quad S_{\text{th}} = \ln D_A. \quad (3)$$

Interestingly, higher order terms in the D_A/D_B -expansion vanish in the replica limit [23, 32–35], and Eq. 3 is exact for arbitrary $N_A \leq N_B$, up to corrections small in $1/D$. (The case $N_A \geq N_B$ follows from exchange $A \leftrightarrow B$.) The result states that to leading order the entropy of the subsystem is that of a maximally random ('thermal') state, S_{th} . The residual term results from wave function interference across system boundaries. Reflecting a common signature of 'interference contributions' to physical observables, it is suppressed by a factor proportional to the Hilbert space dimension.

Regime II & III, energy shell entanglement: — The energy shell now is structured and correlations in the local densities, $\{\nu_n\}$, lead to a much stronger correction to the thermal entropy. Since these contributions come from the identity permutation (do not involve wave function interference), we ignore for the moment $\sigma \neq \text{id.}$, reducing Eq. (2) to $M_r \simeq \sum_l \lambda_{A,l}^r$ with $\lambda_A \equiv \text{tr}_B(\lambda)$. This expression suggests an interpretation of the unit normalized density $\{\lambda_n\}$ as a *spectral measure*, $\sum_n \lambda_n = 1$, $\lambda_n \geq 0$, and of λ_A as the reduced density of system A . With this identification, the entropy,

$$S_A \approx S_{\rho} \equiv \text{tr}_A(\lambda_A \ln(\lambda_A)) \quad (4)$$

becomes the information entropy of that measure.

This is as far as the model-independent analysis goes. Further progress is contingent on two assumptions, which we believe should be satisfied for a wide class of systems in their regimes II and III: First, the exponentially large number of sites entering the computation of the spectral measure justifies a self averaging assumption,

$$\begin{aligned} \sum_{n_X} F(v_{n_X}) &\approx D_X \langle F(v_X) \rangle_X \equiv \\ &\equiv \frac{D_X}{\sqrt{2\pi\Delta_X}} \int dv_X \exp\left(-\frac{v_X^2}{2\Delta_X^2}\right) F(v_X), \end{aligned} \quad (5)$$

where $X = A, B, AB$ stands for the two subsystems, or the full space, respectively, D_X are the respective Hilbert space dimensions, and $\Delta_X = \delta\sqrt{N_X}$. In other words, we replace the sum over site energies by an average over a single variable whose Gaussian distribution follows from the central limit theorem. Second, when integrated against the distribution of subsystem energies v_B , the local DoS at zero energy $E \simeq 0$ acts as a smeared δ -function, setting the additive energy $v = v_A + v_B \simeq 0$, and effectively smoothening the distribution $\lambda_{A,l}$. Since $\kappa \ll \Delta_2 \sim \Delta_B$, the detailed value of the width of the shell, κ , is of no significance in this construction.

Under these assumptions, straightforward computations detailed in the supplementary material yields, e.g.,

the density of states as $D\nu = \sum_{AB} \nu_n \approx D\langle\delta_\kappa(v)\rangle_{AB} = \frac{D}{\sqrt{2\pi N\delta}}$. Applied to the computation of the moments Eq. (2), the averaging procedure obtains the entanglement entropy as [36]

$$S_A - S_{\text{th}} = -\frac{1}{2} \ln\left(\frac{N}{N_B}\right) + \frac{1}{2} \frac{N_A}{N} - \sqrt{\frac{N}{2N_A} \frac{D_A}{2D_B}}. \quad (6)$$

A number of comments on Eq. (6): Provided the above assumptions on the spectral measure hold, the result has the same level of rigor as Page’s formula Eq. (3). The main difference is that (for small subsystems, $N_A \ll N$) the information entropy $S_A - S_{\text{th}} \approx -\frac{1}{4} \left(\frac{N_A}{N}\right)^2$ is exponentially enhanced compared to the correction in Eq. (3). Also note that there is no dependence on the disorder strength (see supplemental material for more details).

Comparison to phenomenological models: — The entanglement entropy (6) is a universal signature of *correlations* (but not the volume) of the energy shell. Conversely, the WFMs, $|\psi_n|^{2q}$, describe the shrinking of the shell volume (but not its correlations). To see that these are independent pieces of information, it is instructive to compare to the random energy model (REM) [42], a phenomenological model replacing the one-body randomness by a set of statistically independent Fock state potentials $\{v_n\}$. For increasing δ , the WFMs diminish as in microscopic models [43]. However, we have verified that the EE of REM states coincides with Page’s Eq. (3). The same result is obtained for sparse random states [22], as even more phenomenological proxies of many body states. What is the origin of the difference to Eq. (6)? A genuine many-body model describes many “bodies”, representing the microscopic degrees of freedom. The Fock space is an outer product over the single body spaces, and the Hamiltonian contains only operators coupling $\mathcal{O}(1)$ of these degrees of freedom. In this sense the REM is *not* a many-body model, since its nonlocal energy operator acts on the products of all (or most) degrees of freedom simultaneously. Specifically, it lacks the principle of energy subsystem additivity $E = E_A + E_B$, required by Eq. (6). In this way, the entanglement entropy becomes a sensitive indicator of whether quantum states are genuine many body states or of different origin.

Regime boundaries: — Upon approaching the boundary to the trivially ergodic regime I, the second condition gets compromised, i.e. the width κ of individual states ceases to be small compared to the statistical fluctuations $\sim \Delta_B$. Leaving a detailed analysis of the crossover region to future work, our numerics below shows a collapse of Eq.(6) to Eq. (3) upon crossing the regime boundary. In the opposite MBL regime IV, eigenstates are concentrated on a small number $\mathcal{O}(1)$ of isolated Fock states, and the concept of an energy shell becomes meaningless: to exponential accuracy in N , remote Fock states, even if they are close in energy, have no common matrix elements with individual eigenstates.

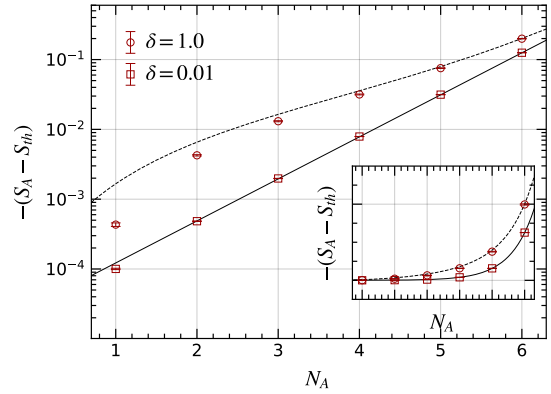


FIG. 2: Numerical entanglement entropies (symbols) vs. analytical (lines) for a system of size $N = 15$ in regime I, $\delta = 0.01$ (solid) and III, $\delta = 1$ (dashed). Inset: linear scale representation of the same data.

The entanglement entropy then scales as $S_A \sim s(\delta/\delta_c)N_A/N$, where s is related to the entropy of the distribution of the localized eigenstate in Fock space. For $1 \ll N_A \ll N$, $S_A \ll 1$ stays small down to $\delta \sim \delta_c$, where it jumps to $S_A \sim N_A$ at the localization transition to regime III.

Numerical analysis: — Fig. (2) shows a comparison of the analytical predictions of Eqs. (3) and (6) with numerical results obtained for the SYK Hamiltonian [36]. In that case, $\hat{H}_4 = \frac{1}{4!} \sum_{i,j,k,l=1}^{2N} J_{ijkl} \hat{\chi}_i \hat{\chi}_j \hat{\chi}_k \hat{\chi}_l$, where $\{\hat{\chi}_l\}$ are Majorana operators [44, 45]. The competing one-body operator reads $\hat{H}_2 = \sum_{i=1}^N m_i (2c_i^\dagger c_i - 1)$, where $c_i = \frac{1}{2}(\hat{\chi}_{2i-1} + i\hat{\chi}_{2i})$ are complex fermion operators defined by the Majoranas [46, 47]. Referring to the supplemental material for details, the agreement is very good, and it becomes better with increasing N_A . (We have no certain explanation for the deviations at the smallest values of N_A .)

Discussion: — In this paper, we applied a combined analysis of the statistics and the entanglement properties of pure quantum states to explore the delocalized phase of disordered many body systems subject to long range correlations. Our analysis supports the view that the appealing concept of “non-ergodic extended states” — adopted including in publications of the present authors [31, 43] — should be abandoned in favor of a qualified interpretation of many body quantum ergodicity. Its key element is the support set $\{n\}$ of states of a given energy, the quantum analog of an energy shell. We have shown how the entanglement properties of pure quantum states reveal ergodicity, and in addition characteristic correlations distinguishing the energy shells of genuine many body systems from those of phenomenological proxies.

What is the scope of the above findings? Referring to the supplemental material for a more detailed discussion,

the freedom to adjust the exponents α, β entering the definition of the model Hamiltonian, implies that our result applies to a wide class of *effectively* long range interacting systems, among them realizations whose interaction operators are short range in a microscopic (“real space”) basis but long range in the eigenbasis of \hat{H}_2 . It is tempting to speculate on generalizations to yet wider system classes. To this end, we note that the derivation of Eq. (6) relies on a number of necessary conditions: subsystem additivity $E \simeq E_A + E_B$ (requiring that the coupling energy between the subsystems is negligibly small in the limit of large system sizes), statistically independent distribution of the the energies $E_{A,B}$, and dependence of the spectral density (measure) on no more than the single conserved quantity, energy. Whether these criteria are not only required but actually sufficient to stabilize the result is an interesting question left for forthcoming research [48]. However, regardless of the scope of Eq. (6), we reason that the combination of wave function statistics and pure state entanglement defines the suitable diagnostic to characterize the ergodic phase of many body quantum chaotic systems.

Acknowledgments: — D. A. H. thanks Vir Bulchandani and Sarang Gopalakrishnan for helpful discussions. F. M. and T. M. acknowledge financial support by Brazilian agencies CNPq and FAPERJ. A. A. acknowledges partial support from the Deutsche Forschungsgemeinschaft (DFG) within the CRC network TR 183 (project grant 277101999) as part of projects A03. The work of M. T. was supported in part by JSPS KAKENHI Grant Numbers JP17K17822, JP20K03787, and JP20H05270. D.A.H. is supported in part by DOE grant DE-SC0016244.

-
- [1] B. L. Altshuler, Y. Gefen, A. Kamenev, and L. S. Levitov, *Quasiparticle Lifetime in a Finite System: A Nonperturbative Approach*, Phys. Rev. Lett. **78**, 2803 (1997).
 - [2] D. Basko, I. Aleiner, and B. L. Altshuler, *Metal-insulator transition in a weakly interacting many-electron system with localized single-particle states*, Ann. Phys. **321**, 1126 (2006).
 - [3] I. V. Gornyi, A. D. Mirlin, and D. G. Polyakov, *Interacting Electrons in Disordered Wires: Anderson Localization and Low-T Transport*, Phys. Rev. Lett. **95**, 206603 (2005).
 - [4] B. L. Altshuler, Y. Gefen, A. Kamenev, and L. S. Levitov, *Quasiparticle Lifetime in a Finite System: A Nonperturbative Approach*, Phys. Rev. Lett. **78**, 2803 (1997).
 - [5] P. G. Silvestrov, *Decay of a Quasiparticle in a Quantum Dot: The Role of Energy Resolution*, Phys. Rev. Lett. **79**, 3994 (1997).
 - [6] P. G. Silvestrov, *Chaos thresholds in finite Fermi systems*, Phys. Rev. E **58**, 5629 (1998).
 - [7] I. V. Gornyi, A. D. Mirlin, and D. G. Polyakov, *Many-body delocalization transition and relaxation in a quantum dot*, Phys. Rev. B **93**, 125419 (2016).
 - [8] I. V. Gornyi, A. D. Mirlin, D. G. Polyakov, A. L. Burin, *Spectral diffusion and scaling of many-body delocalization transitions*, Annalen der Physik (Berlin) **529**, 1600360 (2017).
 - [9] A. Rubio-Abadal, J.-Y. Choi, J. Zeiher, S. Hollerith, J. Rui, I. Bloch, C. Gross, *Many-body delocalization in the presence of a quantum bath*, Phys. Rev. X **9**, 041014 (2019).
 - [10] J.-Y. Choi, S. Hild, J. Zeiher, P. Schauß, A. Rubio-Abadal, T. Yefsah, V. Khemani, D. A. Huse, I. Bloch, C. Gross *Exploring the many-body localization transition in two dimensions*, Science **352**, 1547 (2016).
 - [11] M. Schreiber, S. S. Hodgman, P. Bordia, H. P. Lüschen, M. H. Fischer, R. Vosk, E. Altman, U. Schneider, I. Bloch, *Observation of many-body localization of interacting fermions in a quasi-random optical lattice*, Science **349**, 842 (2015).
 - [12] K. Xu, J. J. Chen, Y. Zeng, Y. R. Zhang, C. Song, W. Liu, Q. Guo, P. Zhang, D. Xu, H. Deng, K. Huang, H. Wang, X. Zhu, D. Zheng, H. Fan, *Emulating Many-Body Localization with a Superconducting Quantum Processor*, Phys. Rev. Lett. **120**, 050507 (2018).
 - [13] P. Roushan, C. Neill, J. Tangpanitanon, V. M. Bastidas, A. Megrant, R. Barends, Y. Chen, Z. Chen, B. Chiaro, A. Dunsworth, A. Fowler, B. Foxen, M. Giustina, E. Jeffrey, J. Kelly, E. Lucero, J. Mutus, M. Neeley, C. Quintana, D. Sank, A. Vainsencher, J. Wenner, T. White, H. Neven, D. G. Angelakis, J. Martinis, *Spectroscopic signatures of localization with interacting photons in superconducting qubits*, Science **358**, 6367 (2017).
 - [14] A. De Luca, B. L. Altshuler, V. E. Kravtsov, and A. Scardicchio, *Anderson Localization on the Bethe Lattice: Nonergodicity of Extended States*, Phys. Rev. Lett. **113**, 046806 (2014).
 - [15] V. E. Kravtsov, I. M. Khaymovich, E. Cuevas, and M. Amini, *A random matrix model with localization and ergodic transitions*, New Journal of Physics **17**, 122002 (2015).
 - [16] B. L. Altshuler, E. Cuevas, L. B. Ioffe, V. E. Kravtsov, *Non-ergodic phases in strongly disordered random regular graphs*, Phys. Rev. Lett. **117**, 156601 (2016).
 - [17] V. E. Kravtsov, B. L. Altshuler, L. B. Ioffe, *Non-ergodic delocalized phase in Anderson model on Bethe lattice and regular graph*, Annals of Physics **389**, 148 (2018).
 - [18] K. S. Tikhonov, and A. D. Mirlin, *Statistics of eigenstates near the localization transition on random regular graphs*, Phys. Rev. B **99**, 024202 (2019).
 - [19] K. S. Tikhonov, and A. D. Mirlin, *Critical behavior at the localization transition on random regular graphs*, Phys. Rev. B **99**, 214202 (2019).
 - [20] K. S. Tikhonov, A. D. Mirlin, *From Anderson localization on Random Regular Graphs to Many-Body localization*, arXiv:2102.05930.
 - [21] K. S. Tikhonov, A. D. Mirlin, *Eigenstate correlations around many-body localization transition*, Phys. Rev. B **103**, 064204 (2021).
 - [22] G. De Tomasi and I. M. Khaymovich, *Multifractality Meets Entanglement: Relation for Nonergodic Extended States*, Phys. Rev. Lett. **124**, 200602 (2020).
 - [23] D. N. Page, *Average entropy of a subsystem*, Phys. Rev. Lett. **71**, 1291 (1993).
 - [24] M. Hague, P. A. McClarty and I. M. Khaymovich, *Entanglement of mid-spectrum eigenstates of chaotic many-body systems – deviation from random ensembles*,

- arXiv:2008.12782 (2020).
- [25] Self consistency enters via the condition $\kappa_n = \pi \sum_m |J_{nm}|^2 \nu_n$, where $|J_{nm}|$ are the matrix elements of the interaction operator (see also Ref. [31]).
 - [26] Random matrix models such as the Rosenzweig-Porter model [27–29], too may develop structured energy shells comprising multiple interlaced “mini bands”. Yet, the absence of a tensor product structure makes these different from the shells of genuine many body systems.
 - [27] N. Rosenzweig, C. E. Porter, ‘*Repulsion of Energy Levels in Complex Atomic Spectra*’, Phys. Rev. **120**, 1698 (1960).
 - [28] E. Cuevas, V. E. Kravtsov, *Two-eigenfunction correlation in a multifractal metal and insulator*, Phys. Rev. B **76**, 235119 (2007).
 - [29] G. De Tomasi, M. Amini, S. Bera, I. M. Khaymovich, and V. E. Kravtsov, *Survival probability in Generalized Rosenzweig Porter random matrix ensemble*, SciPost Phys. **6**, 014 (2019).
 - [30] V. N. Prigodin, *Spatial Structure of Chaotic Wave Functions*, Phys. Rev. Lett. **74**, 1566 (1995).
 - [31] F. Monteiro, T. Micklitz, M. Tezuka, and A. Altland, *A minimal model of many body localization*, Phys. Rev. Research **3**, 013023 (2021).
 - [32] Geoff Penington, Stephen H. Shenker, Douglas Stanford, Zhenbin Yang, *Replica wormholes and the black hole interior*, arXiv:1911.11977.
 - [33] Hong Liu and Shreya Vardhan, *Entanglement entropies of equilibrated pure states in quantum many-body systems and gravity*, Phys. Rev. X Quantum **2**, 010344 (2021).
 - [34] S. K. Foong, S. Kanno, *Proof of Page’s conjecture on the average entropy of a subsystem*, Phys. Rev. Lett. **72**, 1148 (1994).
 - [35] J. Sanchez-Ruiz, *Simple proof of Page’s conjecture on the average entropy of a subsystem*, Phys. Rev. E. **52**, 5653 (1995).
 - [36] See Supplemental Material, where we provide details on the analytical calculation of the entanglement entropy and on the numerical calculations for the SYK model, which includes Refs. [37–41]
 - [37] K. B. Efetov, *Supersymmetry in Disorder and Chaos* (Cambridge Univ. Press, 1999).
 - [38] Alexander D. Mirlin, Phys. Rep. **326**, 259 (2000).
 - [39] A. Altland and D. Bagrets, Nucl. Phys. B **930**, 45 (2018)
 - [40] K.S. Tikhonov and A. D. Mirlin, *Many-body localization transition with power-law interactions: Statistics of eigenstates*, Phys. Rev. B **97**, 214405 (2018).
 - [41] N. Macé, F. Alet, and N. Laflorencie *Multifractal Scalings Across the Many-Body Localization Transition*, Phys. Rev. Lett. **123**, 180601 (2019).
 - [42] C. L. Baldwin, C. R. Laumann, A. Pal, and A. Scardicchio, *The many-body localized phase of the quantum random energy model*, Phys. Rev. B **93**, 024202 (2016).
 - [43] T. Micklitz, F. Monteiro, and A. Altland, *Non-ergodic extended states in the SYK model*, Phys. Rev. Lett. **123**, 125701 (2019).
 - [44] S. Sachdev and J. Ye, *Gapless spin-fluid ground state in a random quantum Heisenberg magnet*, Phys. Rev. Lett. **70**, 3339 (1993).
 - [45] A. Kitaev, <http://online.kitp.ucsb.edu/online/entangled15/kitaev/> /kitaev2/ (Talks at KITP on April 7th and May 27th 2015).
 - [46] A. M. García-García, B. Loureiro, A. Romero-Bermúdez, and M. Tezuka, *Chaotic-Integrable Transition in the Sachdev-Ye-Kitaev Model*, Phys. Rev. Lett. **120**, 241603 (2018).
 - [47] A. R. Kolovsky and D. L. Shepelyansky, *Dynamical thermalization in isolated quantum dots and black holes*, Eur. Phys. Lett. **117**, 10003 (2017).
 - [48] Work in progress.

Supplementary Material to: “Quantum ergodicity in the many-body localization problem”

Felipe Monteiro,¹ Masaki Tezuka,² Alexander Altland,³ David A. Huse,⁴ and T. Micklitz¹

¹*Centro Brasileiro de Pesquisas Físicas, Rua Xavier Sigaud 150, 22290-180, Rio de Janeiro, Brazil*

²*Department of Physics, Kyoto University, Kyoto 606-8502, Japan*

³*Institut für Theoretische Physik, Universität zu Köln, Zùlpicher Str. 77, 50937 Cologne, Germany*

⁴*Department of Physics, Princeton University, Princeton, NJ 08544, USA*

(Dated: February 26, 2022)

In this Supplemental Material, we provide details on the analytical calculation of the entanglement entropy and on the numerical calculations for the SYK model.

PACS numbers: 05.45.Mt, 72.15.Rn, 71.30.+h

ENTANGLEMENT ENTROPY AND LOCAL DENSITY OF STATES

In this section we discuss the derivation of Eq. (2) describing the entanglement entropy in terms of the local density of states. The construction parallels a similar one for the wave functions of single particle systems [1, 2], (see also Ref. [3] for a recent extension to Fock space), and we limit ourselves to an outline of the main construction steps.

Moments of the reduced density matrix from Fock space resolvents:— Working in a first quantized representation — where the Hamiltonian \hat{H} is considered as a high dimensional matrix — our starting point is a representation of the reduced density matrix, $M_r(A) = \langle \text{Tr}_A(\rho_A^r) \rangle$, in terms of retarded/advanced resolvent operators, $G_E^\pm = (E \pm i\eta - \hat{H})^{-1}$. Introducing a formal Lehmann representation in term of exact eigenstates, it is straightforward to verify the likewise exact relation

$$M_r = \frac{(2i)^{r-2}}{\pi\nu_E} \lim_{\eta \rightarrow 0} \eta^{n-1} \langle \text{tr}_A \left((\text{tr}_B[G_E^+])^{r-1} \text{tr}_B[G_E^-] \right) \rangle, \quad (\text{S1})$$

where ν_E is the density of states at energy E .

Construction of the matrix integral:— Following Efetov’s supersymmetry approach [1, 2], we next represent the Green function matrix elements in Eq. (S1) as Gaussian integrals. This representation is obtained from the auxiliary formula $M_{nm}^{-1} = \int D(\bar{\psi}, \psi) e^{-\bar{\psi} M \psi} \psi_m^\sigma \bar{\psi}_n^\sigma$, where M is a general $L \times L$ matrix and the $2L$ dimensional ‘graded’ vector $\psi = (\psi^b, \psi^f)^T$ contains L -commuting components ψ_n^b , and an equal number of Grassmann components ψ_n^f . The double integral over these variables cancels unwanted determinants $\det(M)$, while the pre-exponential factors, either commuting or anti-commuting, $\sigma = b, f$, isolate the inverse matrix element. With the identification $M = \text{diag}(-i[G^+]^{-1}, i[G^-]^{-1}) = \eta - i\sigma_3 \hat{H}$, we are then led to consider the generating function

$$\mathcal{Z}[j] = \int D(\bar{\psi}, \psi) \left\langle e^{-\bar{\psi}(i\eta\sigma_3 - \hat{H})\psi + S_J} \right\rangle, \quad (\text{S2})$$

where we focus on the band center $E = 0$, the average $\langle \dots \rangle$ is with respect to random coefficients of the Hamiltonian \hat{H} , σ_3 is a Pauli matrix distinguishing between advanced and retarded components, and $S_J = \sum_n (j_n \psi_n + \bar{\psi}_n \bar{j}_n)$, with

$$j_n = (\alpha_n \pi^{rr} + \beta_n \pi^{aa}) \otimes \pi^{bb}, \\ \bar{j}_n = (\bar{\alpha}_n \pi^{rr} + \bar{\beta}_n \pi^{aa}) \otimes \pi^{bb}.$$

is a source term from which the required products are obtained by differentiation ($\partial_{\alpha_{n_i}} \equiv \partial_{\alpha_n}|_{n=n_i}$):

$$\sum_{\sigma \in S_{r-1}} G_E^R(n^1, m^{\sigma(1)}) \dots G_E^R(n^{r-1}, m^{\sigma(r-1)}) G_E^A(n^r, m^r) \\ = \prod_{l=1}^{r-1} \partial_{\bar{\alpha}_{m^l}} \partial_{\alpha_{n^l}} \partial_{\bar{\beta}_{m^r}} \partial_{\beta_{n^r}} \mathcal{Z}[j].$$

Here, $\pi^{rr/aa}$ and π^{bb} are projectors onto the subspaces of retarded/advanced and commuting variables, respectively. With this identity, and using the permutation symmetry of Green function matrix elements under trace, we obtain

$$M_r = c_r \lim_{\eta \rightarrow 0} \eta^{r-1} \sum_{\{n^l\}} \prod_{l=1}^{r-1} \partial_{\bar{\alpha}_{m^l}} \partial_{\alpha_{n^l}} \partial_{\bar{\beta}_{m^r}} \partial_{\beta_{n^r}} \mathcal{Z}[j], \quad (\text{S3})$$

where $c_r \equiv (2i)^{r-2}/(\pi\nu_E(r-1)!)$ and the differentiation arguments m^i are fixed as $m^l = (n_A^{l+1}, n_B^l)$, $l = 1 \dots r-1$, and $m^r = (n_A^r, n_B^r)$. Using the notation in the main text this can be summarized as $\mathcal{M}_B^i = \mathcal{N}_B^i$ and $\mathcal{M}_A^i = \mathcal{N}_A^{\tau i}$, where $\tau i = (i+1) \bmod(r)$.

Effective action:— We now average over the random parameters of the interaction Hamiltonian and then apply constructions steps standard in the theory of disordered electronic systems[1, 2] and transferred to the SYK context in Refs. [3, 4]. In regimes I-III, this procedure maps the generating function onto the integral $\mathcal{Z}[j] = \int \mathcal{D}Q e^{-S[Q] + S_J[Q]}$, where $Q = Q \otimes 1_{\text{Fock}}$ is a 4×4 matrix in the spaces of advanced/retarded and commuting/anticommuting indices and

$$S_\eta[Q] = \pi\eta \text{STr}(\dot{\nu} Q \sigma_3), \quad S_J[Q] = -i\pi \text{STr}(\bar{j} \dot{\nu} Q j). \quad (\text{S4})$$

Here ‘STr’ refers to the graded trace over Fock and internal degrees of freedom, and $\hat{\nu}$ is a diagonal matrix in Fock space with the local density of states as its diagonal elements, $(\hat{\nu})_n = \nu_n$.

Moments:—Performing the $2r$ -fold derivative, we arrive at

$$\mathcal{M}_r(A) = c_r \lim_{\eta \rightarrow 0} \eta^{r-1} \sum_{\sigma \in S_r} \sum_N \nu_{n^1} \dots \nu_{n^r} \times \langle Q_{bb}^{rr} \dots Q_{bb}^{rr} Q_{bb}^{aa} \rangle \delta_{\mathcal{N}_A, \sigma \circ \tau(\mathcal{N}_A)} \delta_{\mathcal{N}_B, \sigma(\mathcal{N}_B)}, \quad (\text{S5})$$

where the average $\langle \dots \rangle$ is over the action Eq. (S4). In a final step, we perform the matrix integral to obtain

$$c_r \eta^{r-1} \langle [Q_{bb}^{rr}]^{r-1} Q_{bb}^{aa} \rangle = \frac{1}{(D\nu)^r}, \quad (\text{S6})$$

In this way, the identification of wave function moduli with coefficients of the local density of states fundamental to Eq. (2) of the main text is established.

ENTANGLEMENT ENTROPY IN REGIMES II/III

Leading contribution:— Central to the analysis of the wave function moments is the reduced spectral density, $\lambda_{A,l} = \frac{1}{D\nu} \langle \delta_\kappa(v_l + v_B) \rangle_B$. Performing the Gaussian average Eq. (5) of the main text, we obtain $D\nu = D \langle \delta_\kappa(v) \rangle_{AB} = \frac{D}{\sqrt{2\pi N\delta}}$ and similarly $\lambda_{A,l} = \frac{1}{D_A} \frac{\Delta}{\Delta_B} \exp(-v_l^2/2\Delta_B^2)$.

As discussed in the main text, the leading contribution to the entanglement entropy comes from the identity permutation

$$M_r^{\text{id}}(A) = D_A D_B^r \langle \lambda_A^r \rangle_A. \quad (\text{S7})$$

Substituting the above result for λ_A and performing the Gaussian average, we obtain

$$M_r^{\text{id}}(A) = \frac{D_A^{1-r} N_A^{r/2}}{\sqrt{1 + rN_A/N_B}}. \quad (\text{S8})$$

Subleading contribution:— Single transpositions $\sigma = (ij)$, give the subleading contribution to the entanglement entropy. Inspection of Eq.(2) of the main text (see also the index configuration defined by the right part of the bottom panel of Fig.1) shows that they provide a contribution $M_r^\sigma = \sum_{l_1, l_2} \sum_{m_1, \dots, m_{r-1}} \lambda_{l_1 m_1} \nu_{l_2 m_1} \lambda_{l_1 m_2} \dots \lambda_{l_1 m_{r-1}}$ to the r th moment. Following the same recipe as above, we substitute $\lambda_{l,m} = (D\nu)^{-1} \delta(v_m + v_l)$ and the index summations by Gaussian averages over the energy variables $v_m \rightarrow v_A$ and $v_l \rightarrow v_B$. It is then straightforward to obtain

$$M_r^\sigma = \frac{D_A^{2-r}}{D_B} \frac{N^{r/2}}{\sqrt{N_A}} \frac{N_B^{(2-r)/2}}{\sqrt{2N_B + (r-1)N_A}}. \quad (\text{S9})$$

Noting that there are $\binom{r}{2}$ such terms, the differentiation in r yields the entropy Eq.(6).

Remaining contributions:—In regime I, the leading and subleading contributions discussed above give the Page entropy Eq. (3) in the main text [5]. Permutations that are not the identity or single transpositions vanish. This cancellation has been discussed in the string theory literature [6, 7], and the arguments presented there also apply to regimes II & III. (Basically, the combinatorial factor for contributions with a given number of transpositions are the Narayana numbers and vanish for more than one transposition in the replica limit.) We thus conclude that Eq. (6) describes the entanglement entropy in regime III, at the same level of rigor as Page’s result in regime I.

Comment on crossover to Regime I:—The crossover between Page’s result and our Eq. (5) can be worked out, but requires a more elaborate analysis of above integrals without approximating the local density of states by a δ -function. We leave this analysis for future work.

EXACT DIAGONALIZATION

We numerically calculated the reduced density matrix and the average entanglement entropy for generic eigenstates (in the center of the band) of the SYK Hamiltonian $\hat{H} = \hat{H}_4 + \hat{H}_2$, where $\hat{H}_4 = \frac{1}{4!} \sum_{i,j,k,l=1}^{2N} J_{ijkl} \hat{\chi}_i \hat{\chi}_j \hat{\chi}_k \hat{\chi}_l$, and the free particle contribution [8, 9] $\hat{H}_2 = \frac{1}{2} \sum_{i,j=1}^{2N} J_{ij} \hat{\chi}_i \hat{\chi}_j$. Matrix elements $\{J_{ijkl}\}$ and $\{J_{ij}\}$ are drawn from Gaussian distributions with vanishing mean and variances $\langle |J_{ijkl}|^2 \rangle = 6J^2/(2N)^3$ and $\langle |J_{ij}|^2 \rangle = \delta^2/2N$. The many body band width, Δ_4 , of the interaction operator and the distribution width, Δ_2 , of the on-site random potential then read $\Delta_4 = \sqrt{\frac{3J^2}{4N^3} \binom{2N}{4}}$

and $\Delta_2 = \sqrt{\frac{\delta^2}{2N} \binom{2N}{2}}$, respectively. For our calculations, we generate at least 100 realizations of the Hamiltonians (H_4, H_2) , taking the average of the entanglement entropy over eigenstates corresponding to energies within the middle 1/7th of the spectrum, unless otherwise mentioned. Here, the even and odd fermion parity sectors are diagonalized separately. We further improve the statistics by averaging over all $\binom{N}{N_A}$ Fock space bi-partitions.

In Fig. 2 and Fig. 4 (see below), the error bar shows the standard deviation of the results over the realizations of the Hamiltonians. The two parity sectors are treated as separate samples. We observe an increasing ratio of this error bar to the value of $S_{\text{th}} - S_A$ for diminishing subsystem size N_A . The reason is the exponential diminishing of $S_{\text{th}} - S_A$ with decreasing N_A , which leads to relatively larger numerical fluctuations around this value. We have no certain explanation for the observation that in regime III (and I) results for smallest N_A lie outside the estimated error bar (see also Fig. 3).

A subtlety in these calculations is that the SYK Hamil-

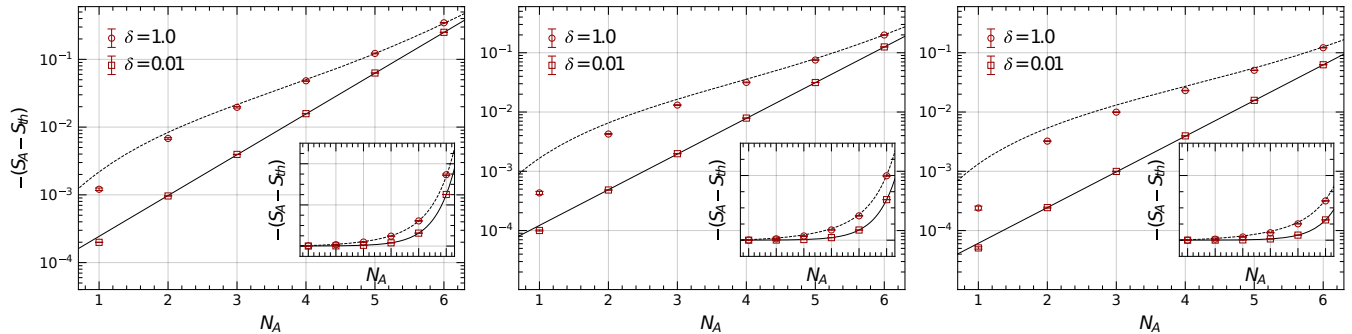


FIG. 3: Numerical entanglement entropies (symbols) vs. analytical (lines) for a system of size $N = 14$ (left), 15 (middle), 16 (right) in regime I, $\delta = 0.01$ (solid) and III, $\delta = 1$ (dashed). Inset: linear scale representation of the same data.

tonian conserves fermion parity. Considering the density matrix ρ defined by an eigenstate with definite parity, the partial trace leads to a block diagonal structure $\rho_A = \text{tr}_B \rho = \begin{pmatrix} \rho_A^e & \\ & \rho_A^o \end{pmatrix}$ with matrices ρ_A^e and ρ_A^o acting in the even and odd fermion parity subspaces of the subsystem A Hilbert space. A trace over the two-dimensional parity sector defines the (normalized) reduced density matrix $\text{tr}_P \rho_A = \rho_A^e + \rho_A^o$. One can then convince oneself that $\text{tr}_P \rho_A$ has the same entropy as the reduced density matrix of a pure state in the 2^{N-1} system with broken fermion parity conservation. This can be also verified by comparing our results in the fully ergodic phase to Page's prediction for a Fock space of dimension $D = 2^{N-1}$, as shown (by the dashed line) in Fig. 2 of the main text.

Variation of entanglement entropy with disorder:— Our analytical analysis predicts the formation of a δ -independent plateau of the entanglement entropy in regime III. In Fig. 4 we show the numerically calculated entanglement entropy for the system sizes $N = 14, 15, 16$, as a function of δ , and for different partitions N_A . For the limited system sizes accessible to exact diagonalization, the observation of a true plateau seems out of reach. However, one can see the formation of the plateau around $\delta = 1$ which becomes more pronounced with increasing N_A and N . At the same time, the value $\delta = 1$ defines the “center” of regime III. This follows from the recent work Ref. [3] by some of the present authors, where the regimes I-IV were characterized in terms of their WFMs. (On the same basis, $\delta = 0.01$ is well within regime I.) While we cannot exclude a coincidence, the respective regime centers as determined by wave function statistics show the best agreement between numerics and analytics for the entropies.

GENERALIZATION

Within the above class of strong interaction coupled models, there is some freedom in the specific realization of the \hat{H}_2 eigenstates. Broadly speaking, this setup is

realized in 3 types of settings: *i)* The system may not have any other geometry beyond that specified by the matrix elements of \hat{H}_4 , as in a SYK model. *ii)* The single-particle eigenstates of \hat{H}_2 may be localized in a d -dimensional real-space, and the couplings in \hat{H}_4 are such that the long-range couplings dominate (e.g., a power-law in space that decays slowly enough) [10]. In these first two cases, as we take the limit of large N , the sparsity of the interactions can be adjusted with N to set α , but we require $\alpha > 0$. *iii)* The single-particle eigenstates of \hat{H}_2 may be all delocalized in real space. In this case, even local interactions couple all-to-all and for density-density interactions, for example, we will have $\alpha = 4$. In all three cases, as we take the limit of large N , the strength of the interactions can be adjusted with N to set β . Our analysis does not apply to models of MBL with only short-range interactions (see e.g. the recent numerical study Ref. [11] on the multifractal scalings across the MBL transition). At the same time, it does not specifically exclude this case, and it seems natural that the ergodicity picture extends to it. However the corroboration of that belief requires further study. (For very recent work on the entanglement entropy of extended random systems, see Ref. [12].)

-
- [1] K. B. Efetov, *Supersymmetry in Disorder and Chaos* (Cambridge Univ. Press, 1999).
 - [2] Alexander D. Mirlin, Phys. Rep. **326**, 259 (2000).
 - [3] F. Monteiro, T. Micklitz, M. Tezuka, and A. Altland, *A minimal model of many body localization*, Phys. Rev. Research **3**, 013023 (2021).
 - [4] A. Altland and D. Bagrets, Nucl. Phys. B **930**, 45 (2018)
 - [5] D. N. Page, *Average entropy of a subsystem*, Phys. Rev. Lett. **71**, 1291 (1993).
 - [6] Geoff Penington, Stephen H. Shenker, Douglas Stanford, Zhenbin Yang, *Replica wormholes and the black hole interior*, arXiv:1911.11977.
 - [7] Hong Liu and Shreya Vardhan, *Entanglement entropies of equilibrated pure states in quantum many-body systems*

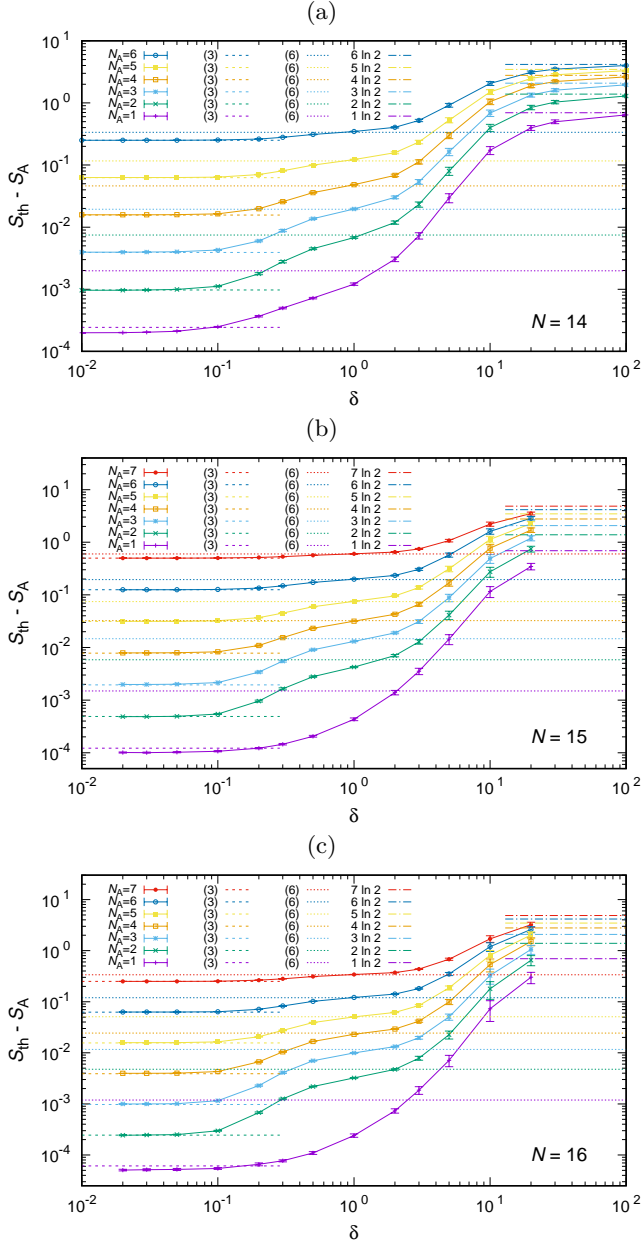


FIG. 4: Entanglement entropy as a function of the disorder strength δ for different partitions N_A , (a) $N = 14$, 104 realizations of the Hamiltonian and 1171 eigenvectors (1/7 of the entire spectrum) are used. (b) $N = 15$, 100 realizations of the Hamiltonian and 100 eigenvectors ($\sim 0.6\%$) are used. (c) $N = 16$, at least 12 realizations of the Hamiltonian and 20 eigenvectors ($\sim 0.06\%$) are used.

- and gravity, Phys. Rev. X Quantum **2**, 010344 (2021).
- [8] A. M. García-García, B. Loureiro, A. Romero-Bermúdez, and M. Tezuka, *Chaotic-Integrable Transition in the Sachdev-Ye-Kitaev Model*, Phys. Rev. Lett. **120**, 241603 (2018).
- [9] A. R. Kolovsky and D. L. Shepelyansky, *Dynamical thermalization in isolated quantum dots and black holes*, Eur. Phys. Lett. **117**, 10003 (2017).
- [10] K.S. Tikhonov and A. D. Mirlin, *Many-body localization transition with power-law interactions: Statistics of eigenstates*, Phys. Rev. B **97**, 214405 (2018).
- [11] N. Macé, F. Alet, and N. Laflorencie *Multifractal Scalings Across the Many-Body Localization Transition*, Phys. Rev. Lett. **123**, 180601 (2019).
- [12] M. Haque, P. A. McClarty and I. M. Khaymovich, *Entanglement of mid-spectrum eigenstates of chaotic many-body systems – deviation from random ensembles*, arXiv:2008.12782 (2020).